

# Neutron scattering and $\mu$ SR investigations of the spin liquid state with quenched disorder in $\text{LuCuGaO}_4$ .

S. Calder,<sup>1</sup> S. R. Giblin,<sup>2</sup> D. R. Parker,<sup>3</sup> P. P.  
Deen,<sup>4</sup> C. Ritter,<sup>4</sup> J. R. Stewart,<sup>4,\*</sup> and T. Fennell<sup>4,†</sup>

<sup>1</sup>*London Centre for Nanotechnology, University College London,*

*17-19 Gordon Street, London WC1H 0AH, UK*

<sup>2</sup>*ISIS Facility, Rutherford Appleton Laboratory,*

*Chilton, Didcot, Oxfordshire OX11 0QX, UK*

<sup>3</sup>*Department of Chemistry, University of Oxford,*

*Inorganic Chemistry Laboratory, South Parks Road, Oxford, OX1 3QR, UK*

<sup>4</sup>*Institut Laue Langevin, BP 156, 6,*

*rue Jules Horowitz, 38042, Grenoble Cedex 9, France*

(Dated: September 2, 2022)

## Abstract

$\text{LuCuGaO}_4$  has magnetic  $\text{Cu}^{2+}$  and diamagnetic  $\text{Ga}^{3+}$  ions distributed on a triangular bilayer. Susceptibility,  $\mu$ SR and neutron scattering measurements show that at low temperature the spins form a short range correlated state with a gapless continuum of excitations. The development of this spin liquid state is strongly reminiscent of that in other two dimensional frustrated magnets and we suggest that it is a generic property of such systems, even surviving in the presence of strong quenched disorder.

## I. INTRODUCTION

$\text{LuCuGaO}_4$  encompasses several topics of interest in condensed matter physics. It has the same crystal structure as the multiferroic  $\text{LuFe}_2\text{O}_4$ <sup>1</sup>: both contain triangular bilayers (Fig. 1), a two-dimensional geometrically frustrated lattice which has so far not been widely studied. Theories of resonating valence bond (RVB) states and other spin liquid ground states<sup>2</sup> typically address low-dimensional frustrated magnets with  $s = 1/2$  and experimental realizations are sought-after for comparison. In  $\text{LuCuGaO}_4$  the magnetic  $\text{Cu}^{2+}$  ions have  $s = 1/2$ , suggesting the possibility of quantum magnetic phenomena, but are strongly diluted by diamagnetic  $\text{Ga}^{3+}$  giving a material with quenched disorder and charge frustration<sup>3,4</sup>.

At a classical level, spins with antiferromagnetic couplings residing on lattices with triangular geometry are frustrated: all pairwise interactions cannot be minimized simultaneously. Many other systems map onto such models, for example the configurations of two cations on such a lattice are identical to those of antiferromagnetically coupled Ising spins on the same lattice<sup>3</sup>, a situation which is known as charge frustration. In  $\text{LuCuGaO}_4$  the  $\text{Cu}^{2+}$  and  $\text{Ga}^{3+}$  cations are distributed over a single site forming well separated triangular bilayers. A single bilayer contains two opposed triangular lattices (see Fig. 1) and the shortest distance between cations is between opposite faces of the bilayer, forming a puckered honeycomb lattice. The combination of honeycomb and triangular geometries may be conveniently viewed as a  $J_1 - J_2$  model on the honeycomb lattice<sup>5,6</sup>, which is a frustrating geometry for magnetic order (see Fig. 1).  $\text{LuCuGaO}_4$  is therefore expected to exhibit both charge and magnetic frustration.

The combination of a frustrating lattice geometry and  $s = 1/2$  is expected to lead to unconventional groundstates such as a spin liquid, as the energy can be further reduced below the classical groundstate by quantum fluctuations (many types and definitions of spin liquids are reviewed by Normand in Ref. 2). Whilst geometrically frustrated magnets have typically been viewed as clean systems in which the effect of frustration can be isolated (in contrast to spin glasses, where structural disorder is also inevitable), it has become apparent that weak structural disorder or non-magnetic impurities can determine the low temperature behaviour of frustrated magnets, where any perturbation of a fragile groundstate is magnified in importance. Examples include the pinning of dimers around non-magnetic impurities in the  $s = 1/2$  kagome Heisenberg antiferromagnet<sup>7-9</sup> or the strain-induced spin glass transition

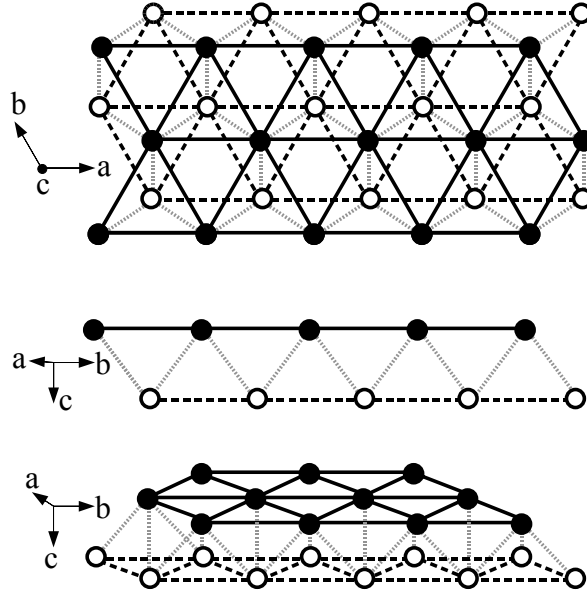


FIG. 1: The topology of the triangular bilayers formed by  $\text{Cu}^{2+}$  and  $\text{Ga}^{3+}$  cations in  $\text{LuCuGaO}_4$ . The two faces of the bilayer are shown in black and white. The shortest bonds (called  $J_1$  in the text) are those that link the two faces of the bilayer forming a puckered honeycomb lattice (grey). Although the honeycomb lattice is bipartite and cation order is therefore possible, the side views (middle and bottom) show that the puckering of this lattice means that such order would cause charge separation across the layer. The bond distance within the faces of the bilayer are slightly longer and form triangular lattices (black and dashes) on which cation (and magnetic) order will be highly frustrated.

in the pyrochlore Heisenberg antiferromagnet with weak bond disorder<sup>10</sup>.

$\text{LuCuGaO}_4$  is a member of the series  $RM\text{M}'\text{O}_4$ , where  $R$  is a small rare earth such as  $\text{Yb}^{3+}$  or  $\text{Lu}^{3+}$ ,  $M$  is a late  $3d$  transition metal cation with  $+2$  charge and  $M'$  is a  $+3$  cation from the late transition metals or main group. Much attention has been focussed on  $\text{LuFe}_2\text{O}_4$ , where charge ordering of  $\text{Fe}^{2+}$  and  $\text{Fe}^{3+}$  is possible and is thought to underlie the multiferroicity<sup>1</sup>. Numerous examples with two different cations have also been characterized. As well as  $\text{LuCuGaO}_4$ ,  $\text{YMnFeO}_4$ ,  $\text{YbMFeO}_4$  ( $M = \text{Mg}, \text{Fe}, \text{Co}, \text{Cu}$ ),  $\text{YbCuGaO}_4$ ,  $\text{LuMFeO}_4$  ( $M = \text{Zn}, \text{Fe}, \text{Co}, \text{Cu}$ ) and  $\text{LuCoGaO}_4$  have all been studied<sup>4,11-25</sup>. Structurally, all are characterized as described above, with randomly distributed  $M$  and  $M'$  ions on the bilayer (the crystal structure is illustrated in Fig. 2 and described in greater detail below). With the exception

of  $RCuGaO_4$  ( $R = Yb, Lu$ )<sup>4</sup> all these materials exhibit a splitting of field cooled and zero field cooled magnetic susceptibilities at temperatures of order 20 K (and in some cases considerably higher), indicative of freezing or spin glass transitions. Previously the most extensively investigated stoichiometry was  $LuMgFeO_4$ <sup>11,18-20,22</sup>. Studies using magnetization measurements, neutron scattering and Mössbauer spectroscopy established that there are short range magnetic correlations associated with frustrated two-dimensional ordering and suggested that random dilution leads to the formation of clusters and two types of site: those lying in the body of clusters and having a full complement of magnetic neighbors, and those lying on extended branches of clusters and having just one or two neighbors.

Previous studies of  $LuCuGaO_4$  also suggest that the copper and gallium ions are randomly distributed on the sites of the bilayer and consequently that  $LuCuGaO_4$  is both spin and charge frustrated<sup>4</sup>. Indeed, despite a Curie-Weiss temperature of  $\theta_{CW} = -69$  K, no magnetic ordering or freezing transition is observed down to 0.4 K where a broad peak in the ac-susceptibility is currently attributed to a spin glass transition<sup>4</sup>. The primary difference between those  $RMM'O_4$  with high temperature freezing transitions and  $LuCuGaO_4$  is the presence of (only)  $s = 1/2$  moments. In this paper we use polarized neutron scattering,  $\mu$ SR and neutron spectroscopy to produce a detailed microscopic characterization of  $LuCuGaO_4$  which suggests that such a state exists, even in the presence of strong structural disorder.

## II. EXPERIMENTAL METHODS

A 20 gram powder sample of  $LuCuGaO_4$  was prepared by reaction of the appropriate stoichiometric quantities of  $Lu_2O_3$  (Alfa Aesar 99.99%),  $CuO$  (Sigma Aldrich, 99.995%) and  $Ga_2O_3$  (Alfa Aesar 99.999%).  $CuO$  and  $Lu_2O_3$  were pre-treated by heating in air for 24 hours at 900 and 1200 °C respectively. The starting materials were ground together, pelletized and heated in air at 1050 °C for a total of 120 hours with 1 intermediate grinding. The field cooled and zero field cooled (FC/ZFC) dc-susceptibility was measured between 1.8 and 300 K in a field of 1000 G using a Quantum Design MPMS-7 SQUID magnetometer.

Neutron powder diffraction patterns were obtained at 70 K and 1.5 K using the D1A diffractometer at the ILL with an incident wavelength of 1.91 Å and standard Orange cryostat. Polarized neutron scattering using the  $xyz$  technique was performed on D7<sup>26</sup> at the ILL using a wavelength of 4.8 Å at temperatures of 0.08, 0.5, 5 and 50 K. Low temperatures were

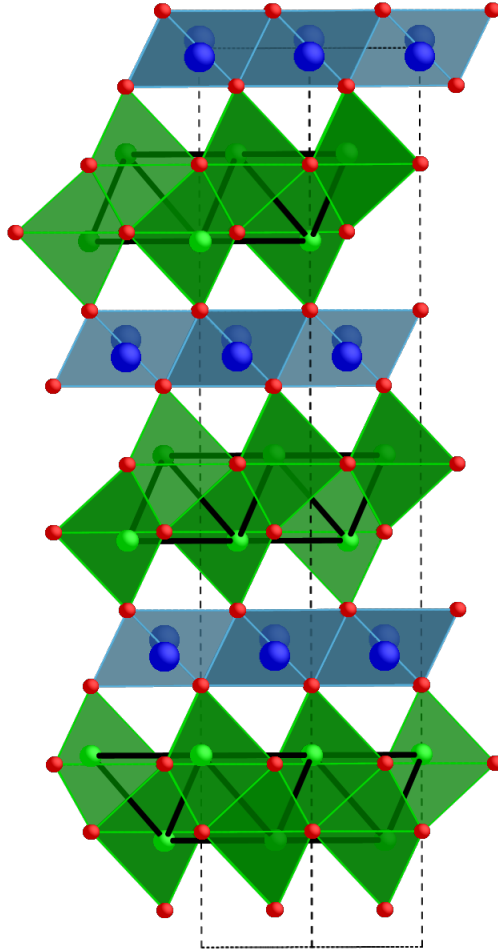


FIG. 2: Crystal structure of  $LuCuGaO_4$  (the  $c$ -axis is vertical on the page, the projection axis is the  $a - b$  diagonal) as obtained from the Rietveld refinement shown in Fig. 3. The bilayers (black bonds) are formed of edge-sharing  $M^{(l)}O_5$  trigonal bipyramids ( $M^{(l)}$  are shown in green,  $O^{2-}$  in red). The bilayers are separated by layers of edge-sharing  $LuO_6$  octahedra. The  $Lu^{3+}$  cations randomly occupy one of two sites displaced from the centre of each octahedron (blue). We suggest (see discussion) that the minimization of the Coulomb interaction amongst the cations is frustrated, and that short range cation correlations are formed amongst the  $Cu^{2+}$  and  $Ga^{3+}$  on the bilayers. The siting of a particular  $Lu^{3+}$  ion would also be controlled by the cation distributions in a triangle on the face of the bilayer immediately above and below the  $LuO_6$  octahedra.

achieved by using a dilution refrigerator insert in a standard Orange cryostat. The sample was contained in a copper can with  $^3He$  exchange gas to provide thermalization below 1 K. An inelastic neutron scattering experiment was carried out on the direct geometry chopper

spectrometer IN4 at the ILL, at temperatures of 1.6, 5 and 50 K using an incident energy of 17 meV.

A zero field and longitudinal field muon spin rotation study was conducted between 0.06 and 50 K with fields up to 2500 G using the MuSR instrument at the ISIS pulsed muon source. The sample was pressed tightly in a silver disk-shaped holder approximately 2 mm deep and cooled with a dilution refrigerator.

### III. RESULTS

#### A. Characterization

We have used powder neutron diffraction and magnetic susceptibility measurements to establish the basic quality of the sample and compare to previous studies. The powder neutron diffraction data show that the sample is phase pure and highly crystalline. The Rietveld method was used to refine three structural models as described in Ref. 4 (see also Ref. 17). The crystal structure has the space group  $R\bar{3}m$  and consists of double layers of edge-sharing  $M^{(l)}O_5$  triangular bipyramids connected by triangular layers of  $RO_6$  octahedra. All three models have  $Cu^{2+}$  and  $Ga^{3+}$  randomly distributed on the  $6c$  site, and differ with respect to the position of  $Lu^{3+}$ . The  $R^{3+}$  ions lie at the centre of distorted octahedra of  $O^{2-}$  ions, directly above and below the centre of triangles of transition metal ions. The simplest model has  $Lu^{3+}$  positioned at  $(0, 0, 0)$ , midway between adjacent bilayers. The more complex models allow anisotropic motion of the  $Lu^{3+}$  ion, or a shift to a lower symmetry site with random half occupation at  $(0, 0, \pm z)$  ( $z = 0.009 \pm 0.0002$ , corresponding to a displacement of 0.22 Å). In this case, the position of each  $Lu^{3+}$  is thought to be controlled by the distribution of cations on the coordinating triangles of adjacent bilayers<sup>4</sup>. As in Ref. 4 the third model provides the best combination of fit and realistic parameters. There is no indication of any structural change between 70 K and 1.5 K. The crystal structure is illustrated in Fig. 2.

We have fitted the inverse magnetic susceptibility to the Curie-Weiss law between 50 K and 300 K, obtaining  $\theta_{CW} = -62.1 \pm 1.8$  K. This is somewhat smaller than the previously reported value (-69 K), but in Ref. 4 the fitting range appears to be restricted to 50 K to 150 K. The magnetic moment obtained from the Curie constant is  $2.2 \pm 0.03 \mu_B$  per  $Cu^{2+}$  (the expected value for  $S = 1/2$  is  $1.7 \mu_B \text{ atom}^{-1}$ ), and the effective moment at 295 K is

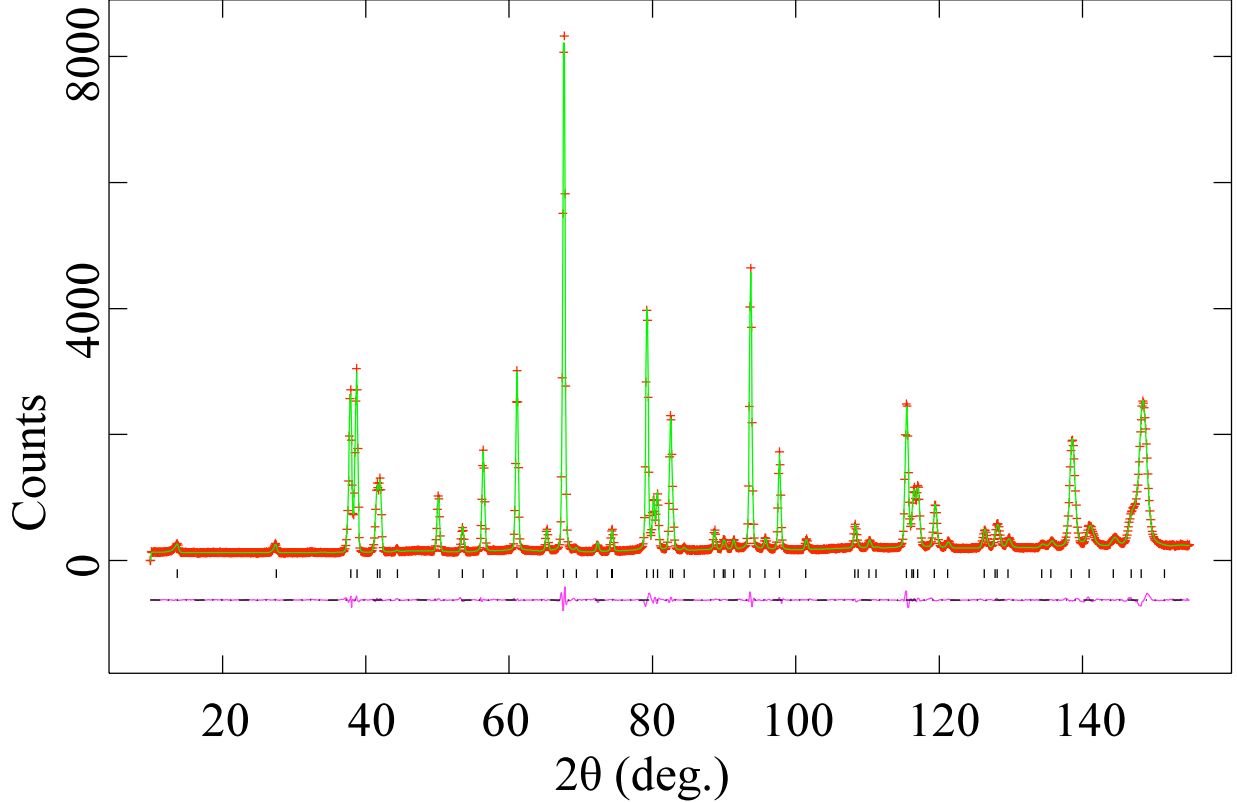


FIG. 3: Neutron powder diffraction at 1.5 K. The experimental data are the red crosses. The fitted line (green) was obtained by using the Rietveld method to refine the model M3 of Ref. 4. The corresponding structure is shown in Fig. 2. The calculated peak positions are indicated by the black ticks and the difference between experimental and fitted profiles by the magenta line.

$\mu_{\text{eff}} \equiv \sqrt{8\chi T} = 1.73 \pm 0.06 \mu_{\text{B}}$  per  $\text{Cu}^{2+}$ . The effective moment falls at low temperature where the inverse susceptibility becomes non-linear, indicating increasing antiferromagnetic spin correlations. At these temperatures there is no discernible splitting between field cooled and zero field cooled measurements.

We have also fitted the entire temperature dependence of the inverse susceptibility with a model of “orphan” spins<sup>27</sup>. This is essentially a Curie-Weiss law with an additional Curie contribution due to isolated spins, which is expected to become dominant at low temperature. Since these spins are, in principle, isolated, they should have  $\theta_{\text{CW}} = 0$ . In this case  $\theta_{\text{CW}1} = -67 \pm 2.9$  K,  $\mu_1 = 2.1 \pm 0.008 \mu_{\text{B}}$ ,  $\theta_{\text{CW}2} = 1.5 \pm 0.8$  K and  $\mu_2 = 0.33 \pm 0.06 \mu_{\text{B}}$ . The downward curving form of  $\chi^{-1}$  is a rather general feature of many frustrated antiferromagnets (see Ref. 28 and references therein) and the reality of the orphan spins remains debatable<sup>27,28</sup>.

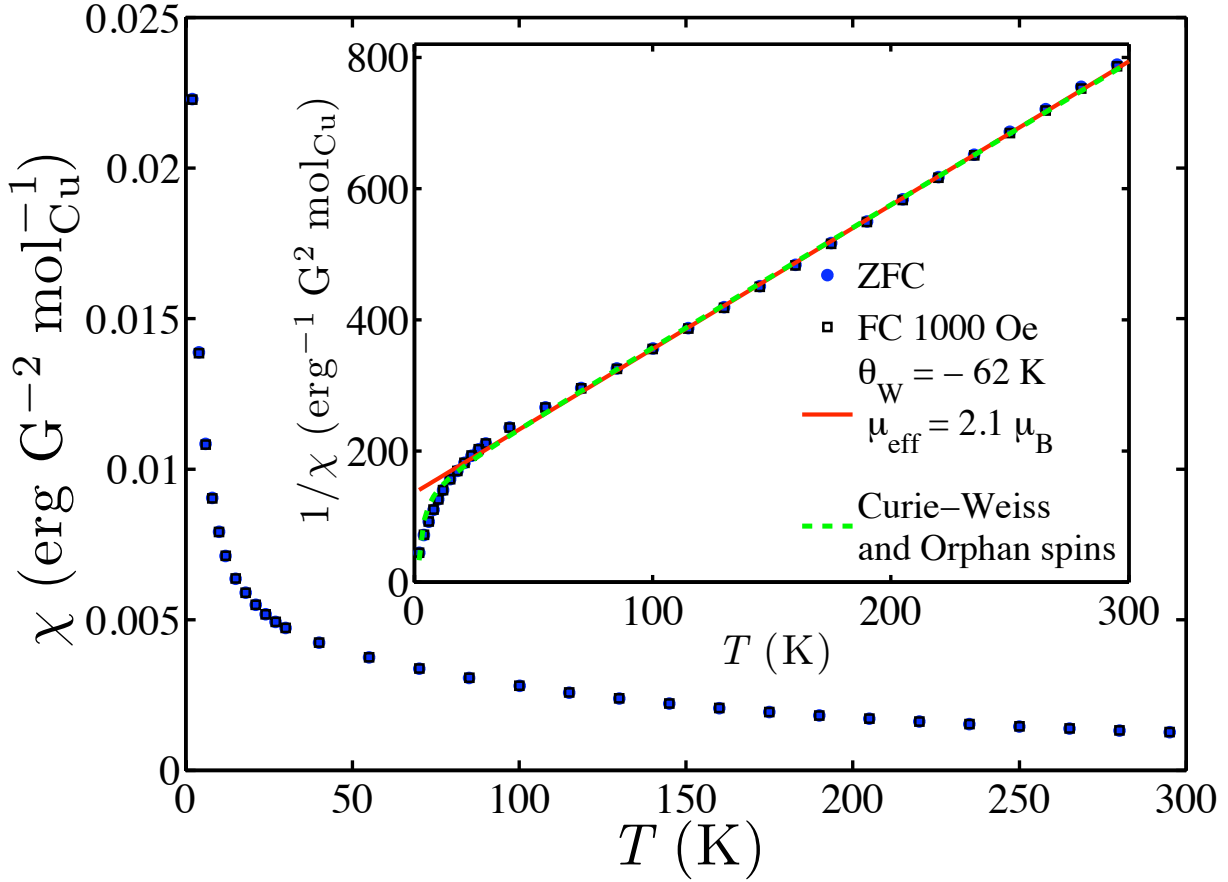


FIG. 4: Susceptibility and (inset) inverse susceptibility for FC dc SQUID measurements at 1000 G. The solid line is a fit to the Curie-Weiss law between 200 and 60 K. ZFC results are identical to FC within experimental error. Also shown is the fit to a model with “orphan” spins<sup>27</sup>.

## B. Polarized Neutron Scattering

The  $xyz$ -polarization analysis technique was used to separate nuclear, spin incoherent and magnetic contributions to the total scattering<sup>26</sup>. The temperatures were selected to compare the paramagnetic regime, where the susceptibility is still described by the Curie-Weiss law (50 K), with the regime in which the inverse susceptibility becomes non-linear (5 K), and the low temperature regime around the proposed spin glass transition. Furthermore, the separation of the contributions allows us to distinguish the origin of any short range order (i.e nuclear or magnetic). The nuclear channel (not shown) contains only Bragg scattering. There is a clear change in magnetic scattering between 50 K and all lower temperatures studied. However, there is no significant change in the low temperature scattering from

5 K down to 0.08 K, in particular between 0.5 and 0.08 K across the proposed spin glass transition, so we have combined the data sets from 0.08, 0.5 and 5 K. As shown in Fig. 5, at 50 K the magnetic scattering can be approximately fitted by the form factor of  $\text{Cu}^{2+}$ , as expected for a paramagnet. At low temperature the form factor response at small  $|Q|$  is suppressed and a broad feature appears, centered around  $1.25 \text{ \AA}^{-1}$ . There is some additional scattering at small  $|Q|$ , above the fitted form factor, which we attribute to air scattering. The magnetic scattering is very weak and has therefore not been observed using conventional neutron powder diffractometers (there is no sign of this feature in Fig. 3 or the earlier study of  $\text{LuCuGaO}_4$ ).

Using an expression for the structure factor of disordered near neighbor antiferromagnetic dimers,

$$I(Q) \propto F^2(Q) \left( 1 - \frac{\sin(Qd)}{Qd} \right) \quad (1)$$

a fit was obtained, as shown in Fig. 5, with  $F^2(Q)$  being the form factor for  $\text{Cu}^{2+}$  and  $d$  the distance between the AFM correlated  $\text{Cu}^{2+}$ . No appreciable difference in the fit is observed if the value of the Cu-Cu distance is  $3.44 \text{ \AA}$  (the distance between Cu-Cu (or Cu-Ga etc) in the triangular layers),  $3.04 \text{ \AA}$  (the Cu-Cu distance across the bilayer), or a weighted average of the two (i.e. due to neighbors on both faces of the bilayer).

This form suggests that there are magnetic correlations between nearest neighbor  $\text{Cu}^{2+}$  ions, which develop in the non-linear region of  $\chi^{-1}$ . The position and form agrees with other members of the series where the larger moments of  $\text{Fe}^{3+}$  or  $\text{Co}^{2+}$  render the diffuse magnetic scattering more readily observable<sup>4,11</sup>. In  $\text{LuMgFeO}_4$ , the dominant feature is also a peak at  $Q \approx 1.25 \text{ \AA}^{-1}$ , but the diffuse scattering profile is much more detailed and correlations could be detected up to the twelfth neighbor shell. This fitting strategy involving further neighbor correlations<sup>11</sup> produced unphysical values for further neighbor correlation functions in  $\text{LuCuGaO}_4$ , so we conclude that the correlations are very short ranged.

We gain no particular understanding of the anomaly previously observed in the susceptibility and specific heat at  $0.4 \text{ K}^4$  as there is no difference between the data measured at 0.08 K and 5 K. This is also a feature of  $\text{LuMgFeO}_4$  where no change in the neutron scattering intensity is seen across the susceptibility cusp<sup>18,21</sup>.

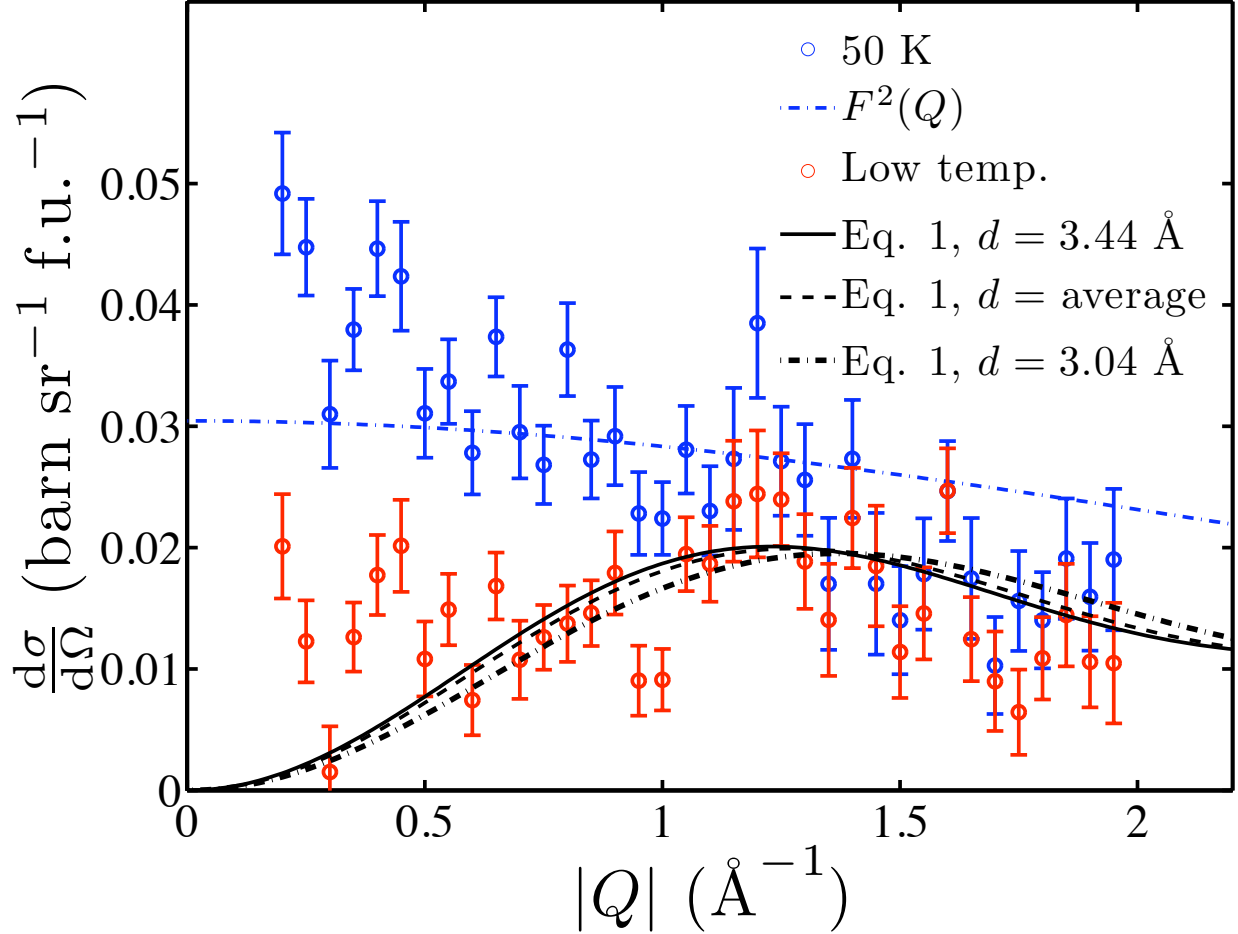


FIG. 5: Separated magnetic component from  $xyz$  polarization analysis experiment. The combined low temperature results (0.08 to 5 K) fit well to a model of nearest neighbor antiferromagnetic correlations. At 50 K  $\text{LuCuGaO}_4$  is paramagnetic and the scattering approximately follows the magnetic form factor for  $\text{Cu}^{2+29}$ .

### C. $\mu\text{SR}$

The development of the spin correlations at low temperature was further investigated using  $\mu\text{SR}$ . The decay of the implanted muon polarization was measured in zero field as a function of temperature and as a function of magnetic field at selected temperatures.  $\mu\text{SR}$  is sensitive to magnetic fluctuations with nuclear and electronic origins on a timescale of  $10^{-5}$  -  $10^{-7}$  seconds. In a paramagnet the electronic fluctuations are mostly very rapid and lie outside the window of the  $\mu\text{SR}$  experiment. Normally in such a situation, any observed relaxation is a consequence of the nuclear component. The nuclear component of the muon

relaxation can usually be decoupled with a field of the order of 10 – 100 G. We have applied longitudinal fields at several temperatures. At 50 K, where the polarized neutron scattering also shows the sample to be paramagnetic, the  $\mu$ SR signal is decoupled in fields of less than 100 G, suggesting the signal is entirely due to relaxation of the nuclear spins. However, at low temperatures, where the polarized neutron scattering shows that spin correlations are developing, a field of 2500 G is insufficient to fully decouple the relaxation. This indicates that at low temperatures there is an increasing electronic contribution, i.e. that as the temperature is decreased, magnetic fluctuations are slowing and falling into the muon time window.

We have therefore fitted the zero-field muon polarization decay for different temperatures (examples are shown in the inset of Fig. 6) with two components: a temperature independent Kubo-Toyabe function to represent the nuclear component, combined with a stretched exponential relaxation of the type  $\exp(-\lambda t)^\beta$ , where  $\beta$  is a constant and  $\lambda$  is the muon depolarization rate. The temperature dependence of  $\lambda$  is shown in Fig. 6. It can clearly be seen that the depolarization rate begins to increase at  $T \approx 10$  K, as the inverse susceptibility becomes non-linear and the peak appears in the diffuse neutron scattering. There is a continual and relatively rapid increase until it reaches a plateau at  $T \approx 0.4$  K, close to the proposed spin glass transition.

#### D. Inelastic neutron scattering

A limited inelastic neutron scattering investigation was also made. The results are shown in Fig. 7. The peak in the magnetic scattering previously described and attributed to nearest neighbor AFM correlations is at  $|Q| \approx 1.25 \text{ \AA}^{-1}$ . In Fig. 7 it can be seen that at 1.7 K inelastic scattering extends from this position. There is no sign of any sharp feature, often visible in powder samples of ordered magnets, even when dispersion surfaces are averaged. The intensity is confined to this single feature, which is rather broad and weakly dependent on the energy transfer. Constant energy cuts further highlight the fact that the magnetic part of the inelastic signal can be fitted by the antiferromagnetic dimer structure factor at all energy transfers (Fig. 7b). A constant  $|Q|$ -cut shows no indication of a gap (Fig. 7c).

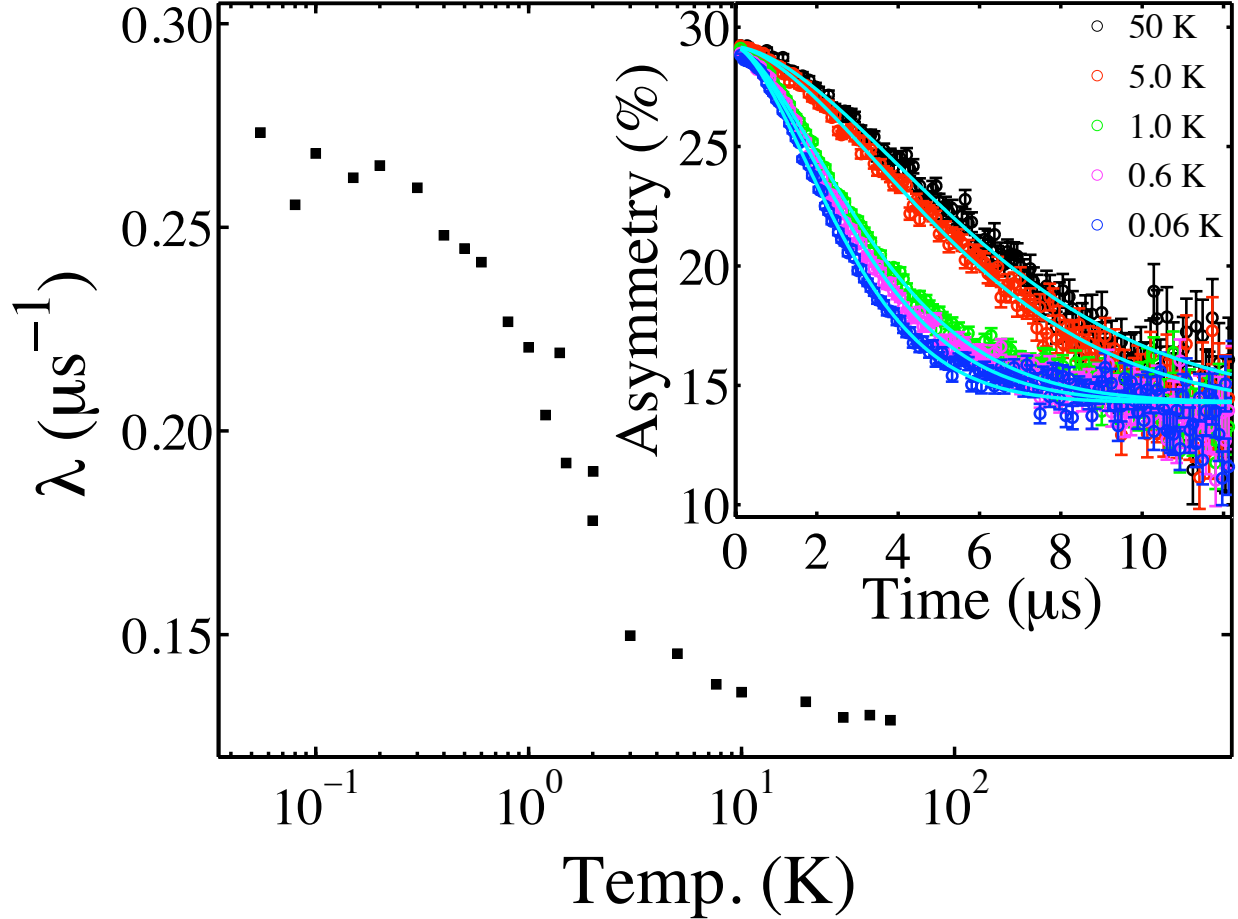


FIG. 6: The muon depolarization rate in zero field as a function of temperature obtained from fits to a temperature independent nuclear response and stretched exponential electronic contribution. Typical fitted muon responses at different temperatures are shown in the inset.

#### IV. DISCUSSION

A spin liquid may be defined by analogy with an actual liquid, as a spin system with short ranged, gapless, dynamic correlations<sup>30</sup>. We seek to make the case that despite strong quenched disorder and the previous description as a spin glass,  $\text{LuCuGaO}_4$  is actually a spin liquid. We first discuss the structural disorder and secondly the liquid-like spin dynamics.

In all the models fitted to the powder diffraction data the  $\text{Cu}^{2+}$  and  $\text{Ga}^{3+}$  ions were treated as randomly distributed on the triangular bilayers, as in all previous works on related materials. However, although the ordering of two different cation species on the triangular bilayer is frustrated (see Fig. 1), a completely random distribution seems unlikely: triangles

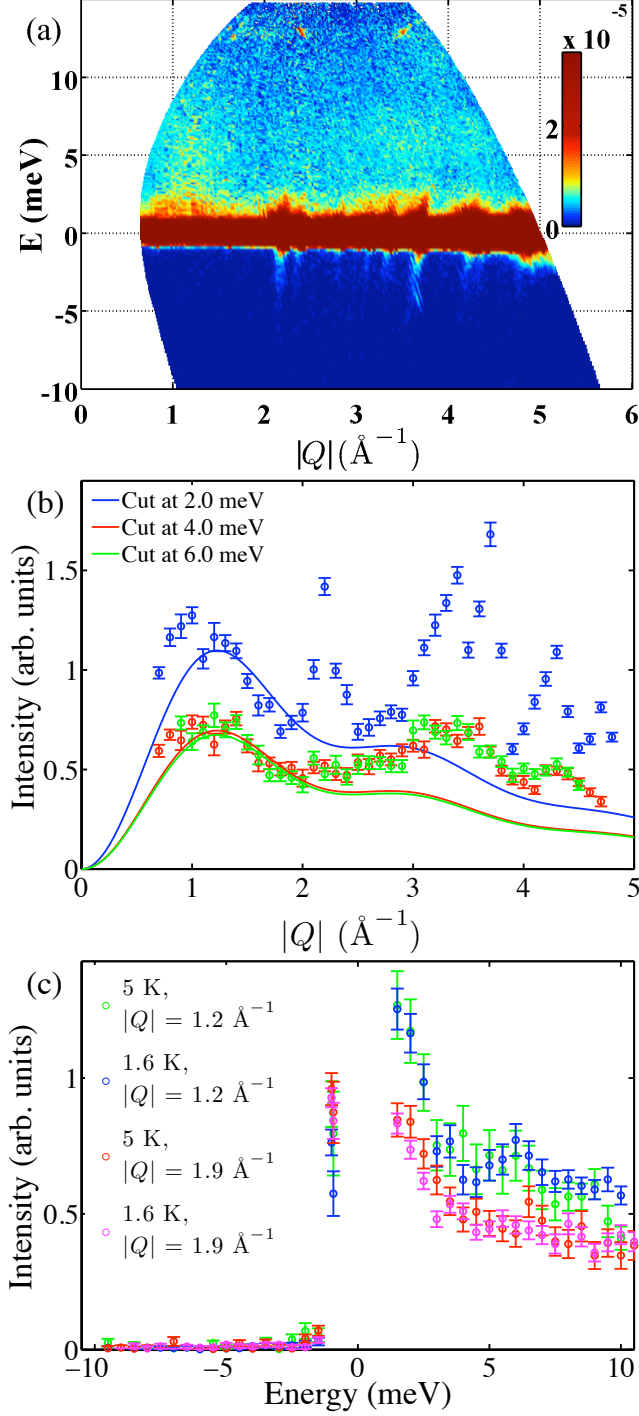


FIG. 7: a:  $S(Q, \omega)$  at 1.7 K with  $E_i = 17$  meV. b: Constant energy cuts through the feature at  $|Q| \approx 1.2 \text{ \AA}^{-1}$  visible in a, with fits to the nearest neighbor AFM structure factor. The peak around  $Q = 1.2 \text{ \AA}^{-1}$  fits well to this model at all energies. There is an increasing phonon contribution at higher  $|Q|$ . c: Cut at  $|Q| = 1.2 \text{ \AA}^{-1}$  and  $1.9 \text{ \AA}^{-1}$  (background).

containing entirely  $\text{Cu}^{2+}$  or  $\text{Ga}^{3+}$  will incur a Coulombic cost. We therefore advance the suggestion that in these materials the cations must be correlated. The nearest neighbor part of the Coulomb energy will be minimized by configurations of the two cations which map to the groundstates of an Ising antiferromagnet on the same lattice, as in other systems with two cation species on a frustrated lattice<sup>3</sup>. Structural diffuse scattering would be expected as a result of these short range correlations. Unfortunately, the scattering lengths of copper and gallium are extremely similar ( $b_{\text{Cu}} = 7.718$  barn and  $b_{\text{Ga}} = 7.288$  barn) so direct detection of short range cation order is effectively impossible.

The importance of this point lies in the resulting quenched disorder configuration. In the case of completely random cations, the topology of the spin system can be compared to percolating clusters, as in Ref. 18. In the case of correlated cations, it appears that the topology of the spin system would take the form of branching loops<sup>31</sup>. Less direct evidence exists for the formation of short-range correlations amongst the cations. For example, one can argue that the existence of two defined positions for the  $\text{Lu}^{3+}$  ions is due to the minimization of electrostatic interactions amongst both the layer and interlayer cations. Without direct evidence for cation correlations, we conclude that the copper and gallium are certainly disordered, and that there is a possibility that they realize a non-trivial network structure.

We turn now to the magnetic correlations. Although we have fitted the peak in the polarized neutron scattering data with the so-called dimer structure factor, we note that this is actually a general description of purely near-neighbor antiferromagnetic correlations. The inelastic scattering data shows that at 1.5 K dynamical correlations exist. The diffuse scattering observed in the polarized neutron scattering experiments may be regarded as integrating over the quasi-elastic part of these fluctuations. The temperature independence of the diffuse peak implies that the correlations remain dynamic at all temperatures measured: if the spins became significantly more static, one would expect to see transfer of spectral weight into the elastic line, certainly resulting in stronger diffuse scattering and possibly a sharper peak shape. The literal interpretation of the dimer structure factor is further precluded as there is no sign of significant singlet formation: the susceptibility does not decrease, there is no clear sign of a singlet-triplet gap in the inelastic neutron scattering data, and the  $\mu\text{SR}$  data implies that the local field in the sample is finite and fluctuating at all measured temperatures.

Canonical spin glasses such as  $\text{AgMn}(0.5 \text{ at. } \%)$  have been extensively investigated by

$\mu$ SR<sup>32</sup>. The depolarization rate increases as the system approaches  $T_g$  but then falls rapidly. In contrast, in  $\text{LuCuGaO}_4$  the depolarization rate increases steadily as the spin correlations build up, but there is no evidence of freezing. We therefore also rule out the existence of a spin glass transition.

The literature provides various examples of similar neutron scattering responses, for example energy independent continua at a particular  $|Q|$  can be found in deuterium jarosite ( $(\text{D}_3\text{O})\text{Fe}_3(\text{SO}_4)_2(\text{OD})_6$ , kagome lattice)<sup>30</sup>; SCGO ( $\text{SrCr}_{8-x}\text{Ga}_{4+x}\text{O}_{19}$ ,  $x = 0.87$ , pyrochlore bilayer)<sup>33</sup>; and  $\text{Y}_{0.5}\text{Ca}_{0.5}\text{BaCo}_4\text{O}_7$  (kagome)<sup>34</sup>. However, the behaviour of  $\text{LuCuGaO}_4$  is most strikingly similar to that of  $\text{ZnCu}_3(\text{OD})_6\text{Cl}_2$  (Herbertsmithite), which is thought to be a structurally perfect  $s = 1/2$  kagome antiferromagnet. In Herbertsmithite,  $\chi^{-1}$  curves below the Curie-Weiss straight line, which may be attributable to Zn-Cu disorder<sup>35,36</sup>. Detailed  $\mu$ SR investigations<sup>37</sup> found a stretched exponential relaxation and increasing depolarization rate at low temperatures which was attributed to slowly relaxing defects, with the remainder of the spins fluctuating too rapidly to be observed by  $\mu$ SR. The neutron scattering response<sup>36</sup> consists of a non-dispersive, gapless feature extending across all observed energies at the wavevector transfer characteristic of the near neighbor distance. It can be fitted by the dimer structure factor at all available energies and measured temperatures between 2 and 120 K. Detailed investigation of the behavior of  $\chi''(Q, T)$  extracted from the neutron scattering data shows that it does not have the expected  $E/T$  scaling expected in theories of spin liquids (this is also the case in deuterium jarosite<sup>30</sup>). While we do not have sufficient data to compare with these observations, we suggest that the overall similarity of the two compounds means that the same physics is realized and may be a general property of two-dimensional,  $s = 1/2$  spin liquids, which is robust to the presence of disorder.

## V. CONCLUSION

We have extended the characterization of  $\text{LuCuGaO}_4$  and shown that it is not a spin glass, but a spin liquid. Although a model of randomly disordered cations is sufficient to explain diffraction data, this may be due to the almost identical scattering lengths of copper and gallium and further investigation of the topological properties of these materials promises to be interesting. At moderate temperatures the spin correlations are shown to be dynamic and gapless. There is a complete absence of spin freezing down to the lowest available

temperature in LuCuGaO<sub>4</sub>, suggesting that the dynamic correlations persist despite the structural disorder. LuCuGaO<sub>4</sub> therefore provides another opportunity to investigate the scaling behaviour of  $\chi(Q, T)$ , demonstrated to be important in other two-dimensional spin liquids.

### Acknowledgments

We thank Sebastien Turc for assistance with cryogenics on D7 and the EPSRC and STFC (UK) for funding.

- 
- \* Now at ISIS Facility, Rutherford Appleton Laboratory, Chilton, Didcot, Oxfordshire OX11 0QX, UK
- † Electronic address: fennell@ill.fr; Began this work at London Centre for Nanotechnology, University College London, 17-19 Gordon Street, London WC1H 0AH, UK
- <sup>1</sup> N. Ikeda, H. Ohsumi, K. Ohwada, K. Ishii, T. Inami, K. Kakurai, Y. Murakami, K. Yoshii, S. Mori, Y. Horibe, et al., *Nature* **436**, 1136 (2005).
- <sup>2</sup> B. Normand, *Contemporary Physics* **50**, 533 (2009).
- <sup>3</sup> P. W. Anderson, *Phys. Rev.* **102**, 1008 (1956).
- <sup>4</sup> R. J. Cava, A. P. Ramirez, Q. Huang, and J. J. Krajewski, *J. Solid State Chem.* **140**, 337 (1998).
- <sup>5</sup> J. B. Fouet, P. Sindzingre, and C. Lhuillier, *Eur. Phys. J. B* **20**, 241 (2001).
- <sup>6</sup> A. Mattsson, P. Fröjdh, and T. Einarsson, *Phys. Rev. B* **49**, 3997 (1994).
- <sup>7</sup> I. Rousochatzakis, S. R. Manmana, A. Läuchli, B. Normand, and F. Mila, *Phys. Rev. B* **79**, 214415 (2009).
- <sup>8</sup> A. Läuchli, S. Dommange, B. Normand, and F. Mila, *Phys. Rev. B* **76**, 144413 (2007).
- <sup>9</sup> S. Dommange, M. Mambrini, B. Normand, and F. Mila, *Phys. Rev. B* **68**, 224416 (2003).
- <sup>10</sup> T. E. Saunders and J. T. Chalker, *Phys. Rev. Lett.* **98**, 157201 (2007).
- <sup>11</sup> A. Wiedenmann, W. Gunsser, J. Rossat-Mignod, and M. O. Evrard, *J. Magn. Magn. Mater.* **31**, 1442 (1983).
- <sup>12</sup> J. Iida, M. Tanaka, and Y. Nakagawa, *J. Phys. Soc. Japan* **59**, 4443 (1990).

- <sup>13</sup> J. Iida, S. Takekawa, and N. Kimizuka, *J. Cryst. Growth* **102**, 398 (1990).
- <sup>14</sup> M. Isobe, N. Kimizuka, J. Iida, and S. Takekawa, *Acta Cryst. C* **46**, 1917 (1990).
- <sup>15</sup> M. Tanaka, J. Iida, and K. Siratori, *Hyperfine Interactions* **54**, 731 (1990).
- <sup>16</sup> J. Iida, M. Tanaka, Y. Nakagawa, S. Funahashi, and Y. Nakagawa, *J. Appl. Phys.* **69**, 5801 (1991).
- <sup>17</sup> T. Matsumoto, N. Mri, J. Iida, M. Tanaka, K. Siratori, F. Izumi, and H. Asano, *Physica B: Condensed Matter* **180-181**, 603 (1992).
- <sup>18</sup> N. Ikeda, K. Kohn, E. Himoto, and M. Tanaka, *J. Phys. Soc. Jpn.* **64**, 4371 (1995).
- <sup>19</sup> M. Tanaka, E. Himoto, and Y. Todate, *J. Phys. Soc. Japan* **64**, 2621 (1995).
- <sup>20</sup> Y. Todate, N. Ohnishi, M. Tanaka, K. Nishiyama, and K. Nagamine, *Hyperfine Interact.* **104**, 375 (1997).
- <sup>21</sup> Y. Todate, C. Kikuta, E. Himoto, M. Tanaka, and J. Suzuki, *J. Phys.: Cond. Matt.* **10**, 4057 (1998).
- <sup>22</sup> Y. Todate, E. Himoto, C. Kikuta, M. Tanaka, and J. Suzuki, *Phys. Rev. B* **57**, 485 (1998).
- <sup>23</sup> T. Sunaga, M. Tanaka, N. Sakai, and Y. Tsunoda, *J. Phys. Soc. Japan* **70**, 3713 (2001).
- <sup>24</sup> H. A. Dabkowska, A. Dabkowski, G. M. Luke, and B. D. Gaulin, *J. Crystal Growth* **234**, 411 (2002).
- <sup>25</sup> K. Yoshii, N. Ikeda, Y. Matsuo, Y. Horibe, and S. Mori, *Phys. Rev. B* **76**, 024423 (pages 12) (2007).
- <sup>26</sup> J. R. Stewart, P. P. Deen, K. H. Andersen, H. Schober, J.-F. Barthélémy, J. M. Hillier, A. P. Murani, T. Hayes, and B. Lindenau, *J. Appl. Cryst.* **42**, 69 (2009).
- <sup>27</sup> P. Schiffer and I. Daruka, *Phys. Rev. B* **56**, 13712 (1997).
- <sup>28</sup> M. Isoda, *J. Phys. Condens. Matter* **20**, 315202 (2008).
- <sup>29</sup> P. J. Brown, *International Tables for Crystallography, vol. C* (Kluwer Academic, Dordrecht, 1992).
- <sup>30</sup> B. Fåk, F. C. Coomer, A. Harrison, D. Visser, and M. E. Zhitomirsky, *EPL* **81**, 17006 (2008).
- <sup>31</sup> S. T. Banks, S. T. Bramwell, T. Fennell, and M. J. Harris, unpublished (2009).
- <sup>32</sup> A. Keren, P. Mendels, I. Campbell, and J. Lord, *Phys. Rev. Lett.* **77**, 1386 (1996).
- <sup>33</sup> H. Mutka, P. Bonnet, C. Payen, C. Ritter, M. Danot, and P. Fabritchini, *Physica B* **350**, e289 (2004).
- <sup>34</sup> W. Schweika, M. Valldor, and P. Lemmens, *Phys. Rev. Lett.* **98**, 067201 (2007).

- <sup>35</sup> J. S. Helton, K. Matan, M. P. Shores, E. A. Nytko, B. M. Bartlett, Y. Yoshida, Y. Takano, A. Suslov, Y. Qiu, J.-H. Chung, et al., *Phys. Rev. Lett.* **98**, 107204 (2007).
- <sup>36</sup> M. A. de Vries, J. R. Stewart, P. P. Deen, J. O. Piatek, G. J. Nilsen, H. M. Rønnow, and A. Harrison, *Phys. Rev. Lett.* **103**, 237201 (2009).
- <sup>37</sup> P. Mendels, F. Bert, M. A. de Vries, A. Olariu, A. Harrison, F. Duc, J. C. Trombe, J. S. Lord, A. Amato, and C. Baines, *Phys. Rev. Lett.* **98**, 077204 (2007).